

# Organic polymer thin-film photo-transistors

Michael C. Hamilton<sup>\*a</sup>, Sandrine Martin<sup>a</sup>, and Jerzy Kanicki<sup>a,b</sup>

<sup>a</sup>EECS Department, The University of Michigan, Ann Arbor, MI, USA 48109-2108;

<sup>b</sup>Center for Polymers and Organic Solids (sabbatical), University of California Santa Barbara, CA, USA 93106-5090

## ABSTRACT

We have investigated the effects of illumination, both broadband and monochromatic, on the electrical performance of organic polymer thin-film transistors (OP-TFTs). In each case, providing the illumination is sufficiently absorbed by the organic polymer, the drain current of a device biased in the OFF-state is significantly increased. We have observed increases in the OFF-state drain current as large as several orders of magnitude depending on the intensity of the incident illumination. Whereas, the drain current of a device biased in the strong accumulation regime is relatively unaffected by the incident illumination. The illumination also serves to decrease the threshold voltage and increase the subthreshold slope, but has little effect on the field-effect mobility of the charge carriers. We explain these effects in terms of the photo-carrier generation in the channel region of the device due to the incident illumination. We have also studied how our OP-TFTs respond to the turn-on and turn-off of gate bias under illumination and to the turn-on and turn-off of illumination at certain gate biases.

**Keywords:** organic polymer, thin-film, transistor, photo-transistor, photosensor, photodetector, photo-field effect

## 1. INTRODUCTION

Electronic and optoelectronic devices, such as organic thin-film transistors (OTFTs), based on semiconducting organic materials, both small molecule and polymer, have shown promise for use in applications such as broad-area flat panel displays and photo-sensor arrays [1-5]. Several groups have proposed or demonstrated all-organic displays constructed in various configurations [6-9]. In applications such as these, the OTFTs will either be integrated with light-emitting devices (as part of the driving circuitry) or will be used to detect the light itself (as a photosensor). Therefore, it is important to understand the effects of illumination on the electrical performance of these devices. In this paper, we present the results of our investigation of the electrical performance of our organic polymer thin-film transistors (OP-TFTs) under broadband and monochromatic illumination. We also present a study of the time response of our OP-TFTs to the turn-on and turn-off of illumination while biased in different operating regimes.

## 2. EXPERIMENTAL DETAILS

### 2.1 Device structure

The structure of the OP-TFT used in this study is shown in Figure 1. The device is in an inverted, co-planar configuration with a defined gate and gate-planarization and has been described previously [10]. The gate definition reduces gate leakage current compared to non-defined gate structures and the gate-planarization allows better step-coverage of subsequently deposited layers and enhanced device performance. The source and drain contacts are sputtered indium tin oxide (ITO) and the gate insulator is PECVD hydrogenated amorphous silicon nitride (a-SiN:H). Benzocyclobutene (BCB) was used as the gate-planarization layer and also serves as a second gate insulator layer. Chromium (Cr) was used for the patterned gate electrode. The organic semiconductor F8T2 [poly(9,9-dioctylfluorene-co-bithiophene) alternating copolymer from The Dow Chemical Company] was used for the active layer (channel region) of the device. A uniform organic polymer film, with an approximate thickness of 1000Å, was achieved by spin-coating from a 1wt% solution of the polymer in mesitylenes. Typical device dimensions are 56 to 116µm and 6 to 56µm for the channel width and length, respectively.

---

\* mchamilt@eecs.umich.edu; phone 1 734 936-0972; fax 1 734 615-2843

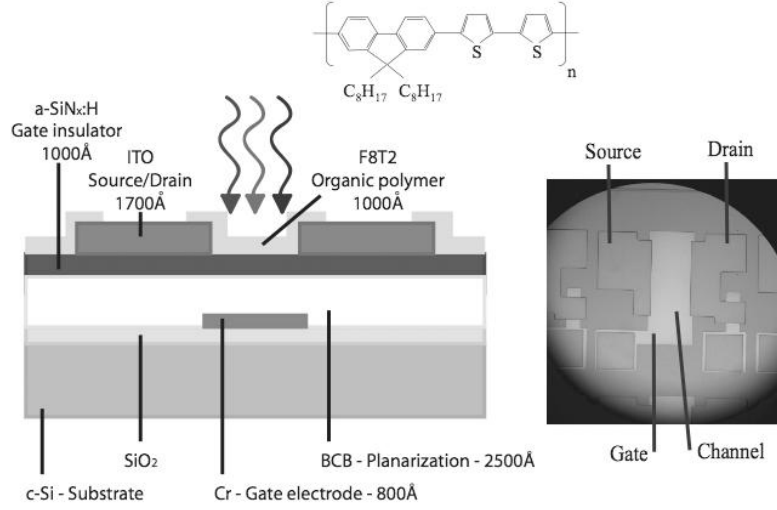


Figure 1. Cross-section of device, chemical structure of F8T2, and picture of device illuminated from the top.

## 2.2 Device operation and parameter extraction

Our devices exhibit p-channel field-effect transistor behavior as can be seen from the transfer characteristics measured in the dark, as shown in Figure 2. The linear regime field-effect mobility and threshold voltage were extracted from the linear regime transfer characteristics using the following equation, based on the MOSFET gradual channel approximation at low drain-to-source voltage [11]:

$$I_D = -\mu_{FElin} C_{ins} \frac{W}{L} (V_{GS} - V_{Tlin}) V_{DS} \quad (1)$$

In this equation,  $\mu_{FElin}$  is the linear regime field effect mobility ( $\text{cm}^2/\text{Vs}$ ),  $C_{ins}$  is the gate insulator capacitance per unit area ( $\text{F}/\text{cm}^2$ ),  $W$  is the channel width of the device,  $L$  is the channel length of the device,  $V_{GS}$  is the applied gate to source bias,  $V_{Tlin}$  is the linear regime threshold voltage and  $V_{DS}$  is the applied drain to source bias. The subthreshold swing was extracted from the linear regime transfer characteristics, in the transition from the OFF-state to the ON-state, using the following equation:

$$S = \left( \frac{d\text{Log}(I_D)}{dV_{GS}} \right)^{-1} \quad (2)$$

In this equation  $S$  is the subthreshold swing ( $\text{V}/\text{decade}$ ). The saturation regime field effect mobility and threshold voltage were extracted from the saturation regime transfer characteristics using the following equation, based on the MOSFET gradual channel approximation [11]:

$$I_D = -\mu_{FEsat} C_{ins} \frac{W}{2L} (V_{GS} - V_{Tsat})^2 \quad (3)$$

In this equation,  $\mu_{FE\ sat}$  is the saturation regime field effect mobility ( $\text{cm}^2/\text{Vs}$ ),  $V_{T\ sat}$  is the saturation regime threshold voltage and the other parameters are the same as described above.

We find values of the linear regime field-effect mobility, threshold voltage, and subthreshold swing to be  $4 \times 10^{-3} \text{ cm}^2/\text{Vsec}$ ,  $-25\text{V}$ , and  $3.0\text{V/decade}$  respectively. Values of saturation field-effect mobility and threshold voltage were found to be  $3 \times 10^{-3} \text{ cm}^2/\text{Vsec}$  and  $-20\text{V}$  respectively.

### 2.3 Experimental set-up

The OP-TFT transfer characteristics ( $I_D$  vs.  $V_{GS}$ , drain current versus gate-to-source voltage) and output characteristics ( $I_D$  vs.  $V_{DS}$ , drain current versus drain-to-source voltage) were measured in the dark and under various levels of broadband and monochromatic illumination at room temperature using a Karl Suss PM8 probe station, an HP4156 semiconductor parameter analyzer, and Interactive Characterization Software (Metrics). We illuminated the devices from the top using a 150W quartz tungsten halogen (QTH) lamp (Mitutoyo microscope lamp) for the broadband source and an optically filtered 200W mercury xenon (HgXe) arc lamp for the monochromatic source. Light from either illumination system is absorbed by the polymer in the range of wavelengths from approximately 400 to 525nm. The incident light intensity of the QTH source was controlled by a potentiometer connected to the QTH supply, providing sufficient control of the illuminance from 0 to 2370lux at the sample surface. The incident wavelength and light intensity from the HgXe source were controlled using optical interference filters (with FWHM < 10nm) and neutral density filters, respectively, providing wavelengths in the range of 435.8 to 690.7nm and intensities in the range of 0 to  $0.5\text{mW}/\text{cm}^2$ . The light was focused to a spot size approximately equal to the area of the device and the entire channel of the device was illuminated as shown in Figure 1. To measure the time dependence of the drain current for various turn-on and turn-off conditions, we used the same set-up as above, with the exception of a Keithley 2400 SourceMeter to bias the gate of the device.

## 3. RESULTS

### 3.1 Effect of broadband illumination on OP-TFT

The electrical performance of our OP-TFTs is changed drastically when the devices are subjected to broadband illumination. The linear regime transfer characteristics of a device in the dark and under illumination are shown in Figure 2. The OFF-state drain current of the device is significantly increased, while the drain current of the device biased in the strong accumulation regime is relatively unaffected. This significant OFF-state drain current increase, when the device is under illumination, is caused by the enhancement of the free carrier density in the channel of the device due to the photo-carrier generation in the polymer. In the strong accumulation regime, though, the gate bias provides sufficient accumulation of free carriers and the effect of the illumination is reduced. We can also see that the OFF-state drain current of the device under illumination is not strongly dependent on  $V_{GS}$ . This may be a useful characteristic for a low power photodetector.

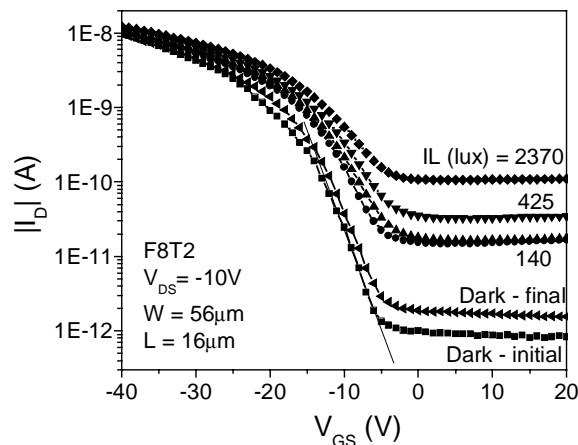


Figure 2. OP-TFT linear regime transfer characteristics in the dark and under various levels of broadband illumination. The line is a fit using equation (2).

In Figure 3, we present the linear plots of the linear regime transfer characteristics. We see, from these plots, that the slopes of the curves in the ON-state, which are proportional to the field-effect mobilities, of all the characteristics are unchanged by the illumination.

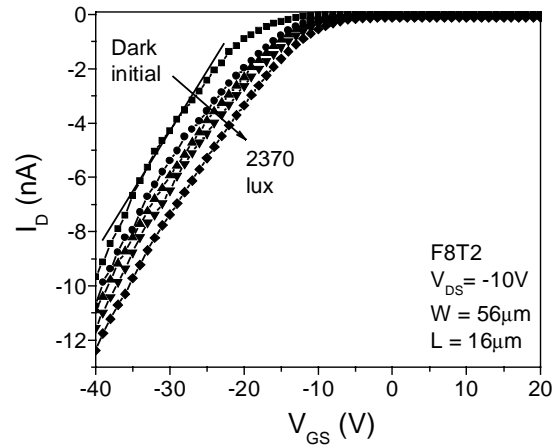


Figure 3. OP-TFT linear regime transfer characteristics in the dark and under various levels of broadband illumination. The line is a fit using equation (1).

Whereas, the threshold voltage (extracted from the curves in Figure 3 using equation (1)) is reduced and the subthreshold swing (extracted from the curves in Figure 2 using equation (2)) increases as the level of illumination is increased, as shown in Figure 4. These effects can be understood in terms of the photo-carrier generation due to the incident illumination. Since the free carrier density in the channel of the device is greatly enhanced by the photo-carrier generation, the gate bias required to bring the device to a certain level of accumulation is effectively reduced for a device under illumination. This is observed as a decrease in the threshold voltage and is shown in Figure 4. The subthreshold swing can be viewed as a measure of the effectiveness or control the gate has on the channel (i.e. a lower subthreshold swing means the gate has better control over the channel). Under illumination, the gate and illumination are both adding to the free carrier density in the channel, therefore the gate loses some the control of the channel compared to operation in the dark. This effect, as shown in Figure 4, is observed as an increase in the subthreshold swing. We have observed similar effects for a-Si:H TFTs in the past [12].

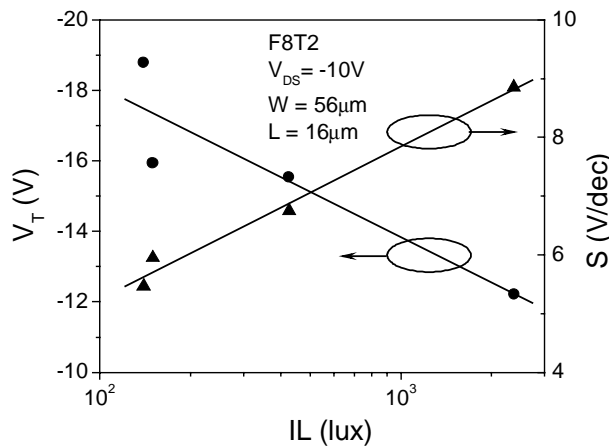


Figure 4. Dependence of threshold voltage and subthreshold swing on level of broadband illumination. Lines are guides to the eye.

It should be noted that the device undergoes full recovery and relaxes back to its original state (i.e. significantly lower OFF-state drain current) after the illumination is removed. This effect can be seen in Figure 2 where  $I_{D\text{ Final}}$  has returned to  $I_{D\text{ Initial}}$ . This recovery takes several minutes, in some cases, when the device is in the air at room temperature.

### 3.2 Effect of monochromatic illumination on OP-TFT

We have also studied the effects of monochromatic illumination on the electrical performance of our OP-TFTs. In these experiments, light from a 200W HgXe lamp was optically filtered using interference and neutral density filters to provide several wavelengths in the range of 435.8 to 690nm. In Figure 5, we present the transfer characteristics of an OP-TFT that was illuminated with a constant optical flux of  $1.3 \times 10^{14}$  photons/sec/cm<sup>2</sup> at 7 wavelengths from 435.8 to 690.7nm. From this figure, we can see that the lower energy light (up to approximately 2.3eV) has a very small effect on the transfer characteristics. On the other hand, light with a higher energy, 2.4 to 2.8eV, has a significant effect on the transfer characteristics. 2.4eV corresponds to the middle of the absorption tail of the F8T2 film we used.

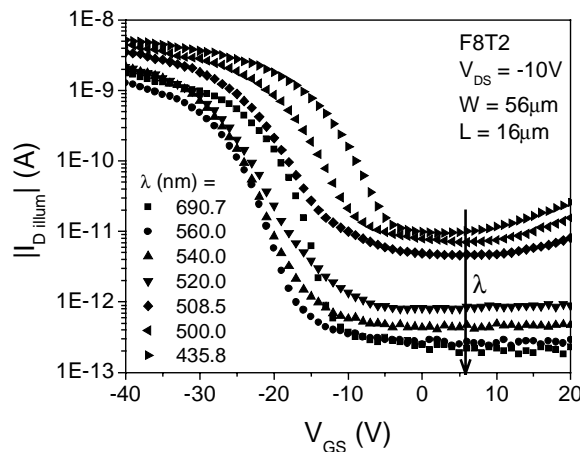


Figure 5. Transfer characteristics of OP-TFT under illumination at different wavelengths for constant optical flux of  $1.3 \times 10^{14}$  photons/sec/cm<sup>2</sup>.

To investigate the effects of monochromatic illumination further, we again measured the transfer characteristics of an OP-TFT under illumination at 460nm, at different intensities. 460nm was chosen because it lies in the absorption peak of F8T2. We can see, from Figure 6, that the effects of the illumination increase (i.e. the OFF-state drain current increases) as the intensity is increased, similar to the broadband illumination.

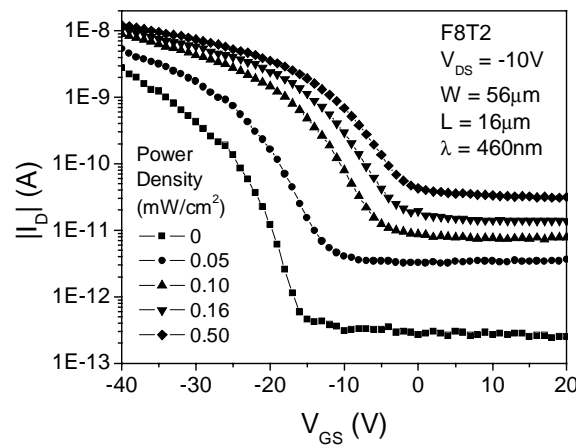


Figure 6. Transfer characteristics of OP-TFT illuminated at different powers at a wavelength of 460nm.

We extracted the threshold voltage and subthreshold swing from the data in Figure 6 using equations (1) and (2). This data is presented in Figure 7. From these plots, we see that the threshold voltage is reduced and the subthreshold swing increases as the illumination intensity increases. The effect of the strongly absorbed monochromatic light is, as expected, similar to the effect of the broadband light. These effects can also be understood using the same explanation as for broadband illumination.

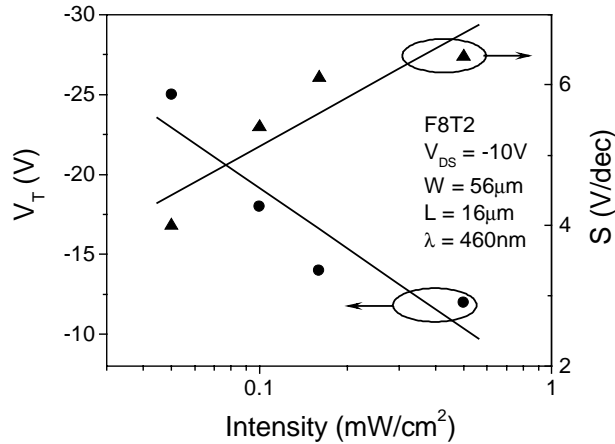


Figure 7. Threshold voltage and subthreshold swing (extracted from Figure 6 using equations (1) and (2)) versus intensity at a wavelength of 460nm. The lines are provided as guides to the eye.

Figure 8 presents a plot of the ratio of drain current under monochromatic illumination to drain current in the dark. In the OFF-state, this ratio is several orders of magnitude and relatively independent of the gate voltage. The peaks in the plots in Figure 8 are due to the reduction of threshold voltage by illumination. This causes the device to be in the ON-state under illumination when it would be in the OFF-state or subthreshold regime for the same gate-to-source bias in the dark.

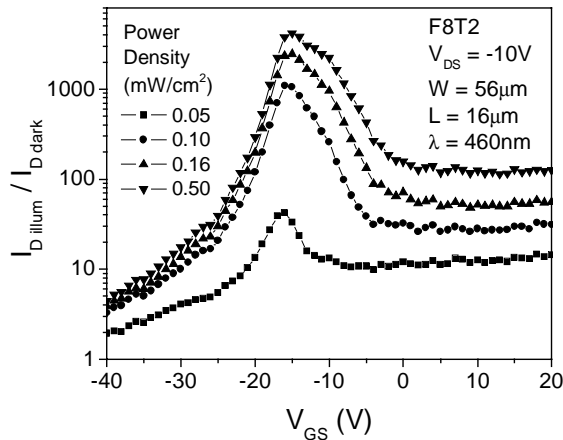


Figure 8. Ratio of drain current under illumination to drain current in the dark for an OP-TFT illuminated at different powers at a wavelength of 460nm (taken from Figure 6.).

### 3.3 Response of OP-TFT to turn-on and turn-off of illumination at certain gate bias

The response of the OP-TFT to the turn-on and turn-off of monochromatic illumination has also been studied. For this experiment, the device was biased at various gate-to-source biases ( $V_{GS}$  0V, -20V, or -40V; corresponding to the OFF-state, subthreshold regime, and strong accumulation regime, respectively) and a drain-to-source bias of -10V. Monochromatic illumination, at a wavelength of 460nm (strongly absorbed) was turned-on for approximately 30 seconds, and then turned-off. The drain current was recorded as a function of time, as shown in Figure 9.

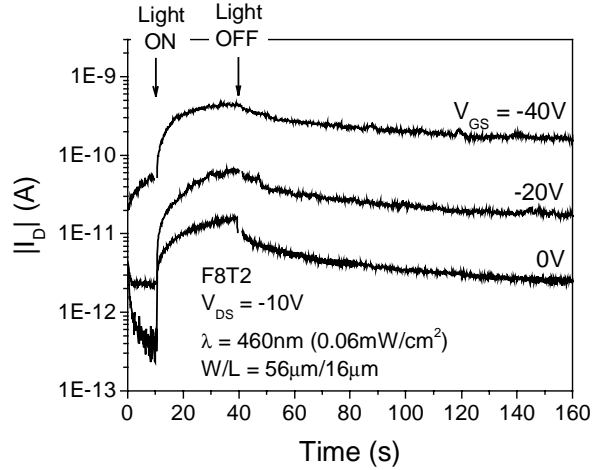


Figure 9. Drain current versus time for the turn-on and turn-off of light at 460nm for an OP-TFT biased at various gate voltages.

We can examine the turn-on responses of the device in each regime in two ways. The first method is to look at the absolute increase ( $I_{D \text{ illum}} - I_{\text{at turn-on}}$ ) for each regime. In this case, since the drain current in the strong accumulation regime is several orders of magnitude larger than the drain current in the OFF-state, we observe that the absolute increase rate, which can be defined as:

$$\frac{d(I_{D \text{ illum}} - I_{D \text{ at turn-on}})}{dt} \quad (4)$$

is larger in the strong accumulation regime compared to the absolute increase rate in the OFF-state. Another method of comparison of the responses of the device in the different regimes is to look at the relative increase ( $I_{D \text{ illum}} / I_{\text{at turn-on}}$ ). In Figure 10 we present the drain current, during the time following the turn-on of illumination, normalized to the drain current at the time the illumination was turned on. From this figure, we see that the slopes of the plots are similar, and therefore the relative increase rates, which can be defined as:

$$\frac{d(I_{D \text{ illum}} / I_{D \text{ at turn-on}})}{dt} \quad (5)$$

are similar for all device operation regimes.

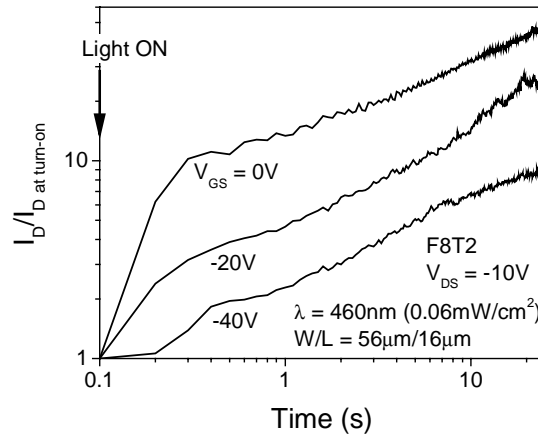


Figure 10. Drain current versus time normalized to drain current at the turn-on of light at 460nm for an OP-TFT biased at various gate voltages. Curves have been shifted in time, to facilitate plotting on log-log scales.

We can apply similar methods to the analysis of the turn-off response of the device in different operating regimes. Figure 11 shows the drain current, during the time following the turn-off of illumination, normalized to the drain current at the time the illumination was turned off. From this figure, we observe that the illumination turn-off response of the device is dependent on the gate-to-source bias (operating regime) and that it has a faster relative decrease rate, defined as:

$$\frac{d(I_{Dillum} / I_{D at turn-off})}{dt} \quad (6)$$

in the OFF-state compared to the relative decrease rate in the strong accumulation regime.

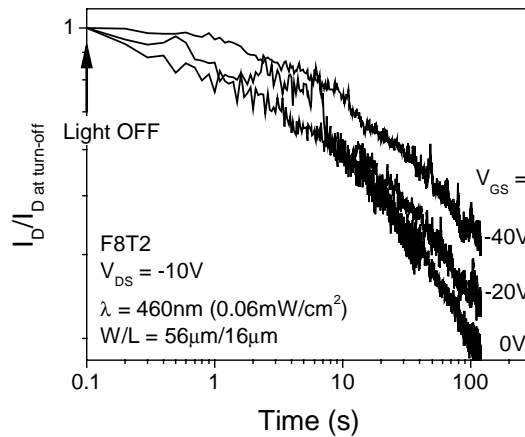


Figure 11. Drain current versus time normalized to drain current at the turn-off of light at 460nm for an OP-TFT biased at various gate voltages. Curves have been shifted in time, to facilitate plotting on log-log scales.

Currently, experiments are underway to aid in the understanding and explanation of the turn-on and turn-off responses of our device.

## 4. CONCLUSIONS

We have studied the electrical performance of our OP-TFTs under broadband and monochromatic illumination. In each case, the major effect of the absorbed light is a significant increase in the OFF-state drain current, while the drain current in the strong accumulation regime remains relatively unchanged. We have also shown that these effects are strongly dependent on the level of illumination (for both broadband and monochromatic light) and the wavelength of the incident illumination (for monochromatic light). Weakly absorbed light, with energy below the optical-gap, has almost no effect on the electrical characteristics of the OP-TFT. In the OFF-state, the response of the device to the illumination (both broadband and monochromatic) is gate voltage independent. Therefore, when operated in the OFF-state, this device could be used as a low power photosensor. The time response of our OP-TFT to the turn-on and turn-off of illumination has also been reported. We have shown that the response can be examined in two ways: absolute and relative. Each method gives different results for the response to illumination turn-on. The absolute increase rate is fastest for a device biased in the strong-accumulation regime, while the relative increase rate appears to be independent of gate-bias. For the turn-off time response, the relative decrease rate increases as we bias the device from the OFF-state into the strong accumulation regime. In all cases, we have observed full recovery of the device after the illumination is removed.

## ACKNOWLEDGEMENTS

One of the authors (MCH) was supported through a National Defense Science and Engineering Graduate fellowship (AFOSR) administered by ASEE. One of us (JK) would like to thank Prof. A. Heeger (UCSB, CA) for his support. We would also like to thank The Dow Chemical Company for the organic polymer (F8T2) used in this study.

## REFERENCES

- [1] G. Horowitz, "Organic Field-Effect Transistors", *Adv. Mat.*, **vol. 10**, pp. 367-377, 1998.
- [2] C.D. Dimitrakopoulos and D.J. Mascaro, "Organic thin-film transistors: A review of recent advances", *IBM J. of Res. and Dev.*, **vol. 45**, pp. 11-27, 2001.
- [3] H.E.A. Huitema, G.H. Gelinck, J.B.P.H. van der Putten, K.E. Kuijk, C.M. Hart, E. Cantatore, P.T. Herwig, A.J.J.M van Breemen, and D.M. de Leeuw, "Plastic transistors in active-matrix displays", *Nature*, **vol. 414**, pp. 599, 2001.
- [4] K.S. Narayan, A.G. Manoj, Th.B. Singh, A.A. Alagiriswamy, "Novel strategies for polymer based light sensors", *Thin Sol. Films*, **vol. 417**, pp. 75-77, 2002.
- [5] K.S. Narayan and N. Kumar, "Light responsive polymer field-effect transistor", *Appl. Phys. Lett.*, **vol. 79**, pp. 1891-1893, 2001.
- [6] T.N. Jackson, Y. Lin, D.J. Gundlach, and H. Klauk, "Organic thin-film transistors for organic light-emitting flat-panel display backplanes", *IEEE J. Select. Topics Quantum Electron.*, **vol. 4**, pp. 100-104, 1998.
- [7] H. Sirringhaus, N. Tessler, and R.H. Friend, "Integrated Optoelectronic Devices Based on Conjugated Polymers", *Science*, **vol. 280**, pp. 1741-1743, 1998.
- [8] K. Kudo, D.X. Wang, M. Iizuka, S. Kuniyoshi, and K. Tanaka, "Organic static induction transistor for display devices", *Synth. Met.*, **vol. 111-112**, pp. 11-14, 2000.
- [9] S.W. Pyo, Y.M. Kim, J.H. Kim, J.H. Shim, L.Y. Jung, and Y.K. Kim, "An organic electrophosphorescent device driven by all-organic thin-film transistor using photoacryl as a gate insulator", *Cur. Appl. Phys.*, **vol. 2**, pp. 417-419, 2002.
- [10] S. Martin, J.Y. Nahm, and J. Kanicki, "Gate-planarized organic polymer thin-film transistors", *J. of Elec. Mat.* **vol 31**, pp. 512 (2002).
- [11] R.F. Pierret, *Semiconductor Device Physics*, (Addison-Wesley, Reading, 1996) p. 620.
- [12] J.D. Gallezot, S. Martin, and J. Kanicki, "Photosensitivity of a-Si:H TFTs", *Proceedings of the IDRC 2001*, pp. 407, 2001.